Changes in the Timing of Phytoplankton Blooms Related to Diminished Ice Cover in the Arctic

Article · December 2010

CITATIONS
0

READS
187

4 authors, including:

Mati Kahru
University of California, San Diego
150 PUBLICATIONS **8,182** CITATIONS
SEE PROFILE

Vanda Brotas
University of Lisbon
127 PUBLICATIONS **2,774** CITATIONS
SEE PROFILE

Global Change Biology

Global Change Biology (2010), doi: 10.1111/j.1365-2486.2010.02312.x

Are phytoplankton blooms occurring earlier in the Arctic?

M. KAHRU*, V. BROTAS†, M. MANZANO-SARABIA‡ and B. G. MITCHELL*

*Scripps Institution of Oceanography, University of California San Diego, La Jolla, California, USA, †Centre of Oceanography, Faculdade de Ciências da Universidade de Lisboa, Lisboa, Portugal, ‡Facultad de Ciencias del Mar, Universidad Autónoma de Sinaloa, Mazatlán, Sinaloa, México

Abstract

Time series of satellite-derived surface chlorophyll-*a* concentration (*Chl*) in 1997–2009 were used to examine for trends in the timing of the annual phytoplankton bloom maximum. Significant trends towards earlier phytoplankton blooms were detected in about 11% of the area of the Arctic Ocean with valid *Chl* data, e.g. in the Hudson Bay, Foxe Basin, Baffin Sea, off the coasts of Greenland, in the Kara Sea and around Novaya Zemlya. These areas roughly coincide with areas where ice concentration has decreased in early summer (June), thus making the earlier blooms possible. In the selected areas, the annual phytoplankton bloom maximum has advanced by up to 50 days which may have consequences for the Arctic food chain and carbon cycling. Outside the Arctic, the annual *Chl* maximum has become earlier in boreal North Pacific but later in the North Atlantic.

Keywords: arctic, climate change, ocean color, phenology, phytoplankton blooms, remote sensing

Received 26 April 2010; revised version received 30 June 2010 and accepted 9 August 2010

Introduction

Both satellite and *in situ* studies on land have shown that in many temperate ecosystems the spring onset of vegetation greenness has advanced, the growing season has lengthened, and both these changes are correlated with rising temperatures (Myneni *et al*., 1997; Cleland *et al*., 2007). A limited number of corresponding observations using phytoplankton species in the ocean (Edwards & Richardson, 2004; Winder & Schindler, 2004; Thackeray *et al*., 2008) have also been able to show changes in the timing of annual phenomena but others (Winder & Cloern, 2009) question the ability to detect climate driven trends in phytoplankton communities due to their high spatio-temporal variability. Satellite-derived time series of chlorophyll-*a* concentration (*Chl*, mg m^{-3}), used as a proxy for phytoplankton biomass, have shown trends of increased phytoplankton bloom magnitude in coastal and shelf areas (Kahru & Mitchell, 2008; Kahru *et al*., 2009) as well as multidecadal and interannual oscillations in oceanic patterns of *Chl* and sea surface temperature (Behrenfeld *et al*., 2006; Martinez *et al*., 2009). The detection of changes in the timing of blooms is complex due to the various shapes of the annual cycle in phytoplankton biomass and the high variability in the oceanic time series (Vargas *et al*., 2009).

Phytoplankton blooms stimulate the production of zooplankton which, in turn, provides forage for larval fish (Platt *et al*., 2003). The height and timing of the annual *Chl* maximum are a result of many interacting processes (Siegel *et al*., 2002). It appears that secondary producers, such as shrimp, may have adapted their egg hatching times to the phytoplankton spring bloom (Koeller *et al*., 2009). The match or mismatch between the reproductive cycles of marine organisms and their food may partly determine the year class strength (Cushing, 1990). Here, we use satellite-derived *Chl* to objectively map changes in the timing of the annual phytoplankton maxima, with an emphasis on the Arctic Ocean and the adjacent boreal oceans. We acknowledge that the annual cycle can have a multitude of shapes (cf. Vargas *et al*., 2009; Platt *et al*., 2010); however, as a first approximation, we search for trends in the timing of the annual maximum without considering the shape of the annual cycle.

Correspondence: M. Kahru, Scripps Institution of Oceanography, University of California San Diego, La Jolla, CA, USA, tel. +1 858 534 8947, fax +1 858 822 0562, e-mail: mkahru@ucsd.edu

Data and methods

Satellite-derived Level-3 (i.e. binned and mapped) data sets of chlorophyll-*a* concentration (*Chl*, mg m^{-3}) were obtained from NASA's Ocean Color website (http://oceancolor.gsfc.nasa.gov/) and the European Space Agency's GlobColour project (http://www.globcolour.info). Daily composite concentrations of *Chl* using standard Case 1 water algorithms (O'Reilly *et al*., 1998; Morel & Maritorena, 2001) were obtained. Any single ocean color sensor has a limited daily coverage resulting from gaps between the swaths, sun glint and cloud cover. Merging data from multiple sensors – if data

from more than one sensor are available – will increase the coverage due to the combination of patchy and uneven daily coverage from sensors viewing the ocean at slightly different times and geometries. Compared with data from individual sensors, the merged products from three sensors (SeaWiFS, MERIS, MODIS-Aqua) have approximately twice the mean global coverage and lower uncertainties in the retrieved variables (Maritorena *et al*., 2010). We therefore used *Chl* data merged by GlobColour from multiple sensors (SeaWiFS, MERIS, MODIS-Aqua) with weighted averaging (http://www.globcolour.info/CDR_Docs/GlobCOLOUR_PUG.pdf) whenever possible (April 2002–December 2009) and data from individual sensors (OCTS, November 1996–June 1997; SeaWiFS, September 1997–March 2002) during periods when only the single sensor data were available. While small but systematic differences exist between the products of individual sensors, the large scale *Chl* distributions produced by the major ocean color missions are consistent over a wide range of conditions (Morel *et al*., 2007; Djavidnia *et al*., 2010). We expect that the merged product based on standard Case 1 water algorithms has better coverage, higher quality and lower uncertainty than the data from individual sensors, similar to when using the semianalytical model-based data merger (Maritorena *et al*., 2010). As we are using the timing of the annual *Chl* maximum and not the actual *Chl* value, small errors in *Chl* estimates are expected to have a minor effect on our results. The latest versions of the data available at the time were used (e.g. reprocessing 2009.1 for SeaWiFS data, reprocessing 2007 for the merged data and the other sensors).

Daily *Chl* datasets were composited into 5-day time series spanning 13 years (1997–2009) with approximately 25 km spatial resolution. The year day of the annual *Chl* maximum was found as the middle day of the 5-day composite with the annual maximum *Chl* for each pixel. As an additional characteristic of the day of the *Chl* maximum, the day length of that day was calculated as the time interval between sunset and sunrise (using the code available at http://personal.inet.fi/cool/jjlammi/rscalc.c).

Sea ice concentrations were obtained from the Nimbus-7 SMMR and DMSP SSM/I passive microwave data using the NASA Team algorithm (Cavalieri *et al*., 1996, updated 2008). Monthly ice concentrations were used to evaluate trends and daily ice data to evaluate the timing of changes in ice concentration.

The existence of trends and their significance was evaluated with the Sen slope estimator (Sen, 1968; Gilbert, 1987). The time series used here are noisy and non-Gaussian and therefore the use of a nonparametric method is preferred. Sen slope is a nonparametric estimate of the slope that is derived by computing slopes of all possible points of a time series and then using the median of these slopes as an estimate of the overall slope. The nonparametric Mann–Kendall test was used to evaluate the statistical significance of the trend according to Salmi *et al*. (2002).

Results

First, we established the median timing of the annual *Chl* maximum for the period from 1997 to 2009 (Fig. 1). In temperate waters, the annual *Chl* maximum typically represents the phytoplankton spring bloom but it can also represent the fall bloom or episodic blooms. The spatial pattern in the timing of the annual *Chl* maximum is mostly zonal but with striking patchiness in some areas, such as South-East Asia and the Pacific and Atlantic oceans off Central America. Changes in the zonal bands are not monotonic along the meridians. For example, in the Northern Pacific, along the 170°W meridian (Fig. 1b), the year day of *Chl* maximum increases from about 100 (April) just north of the equator to about 200 (July) between 10 and 25°N, then drops to about 50 (February) in the band centered at about 30°N, increases to about 250 (September) in a band centered at about 46°N, drops again to about 150 (May–June) in the Bering Sea and increases again to about 220 (August) in the Arctic Ocean north of the Bering Strait. In the North Atlantic, the gradual increase in the year day with latitude northwards from 20°N is interrupted at about 55°N, after which it drops when moving north near Greenland (Fig. 1c). In the North Pacific, the band of late summer (July–September, green to orange colors) blooms at about 40–55°N is a dominant feature but the corresponding late summer blooms in the North Atlantic are earlier (July–August, green colors) and spatially fragmented.

Time series of the year day of the annual *Chl* maximum are noisy and, outside of the high latitude regions, can include the whole range of year days from 1 to 365 or 366. This can produce erratic regressions with spurious slopes and false positives (Fig. 2a). We therefore used a related variable, the day length of the annual *Chl* maximum day (Fig. 2b), as a secondary (proxy) variable to help detect and confirm changes in the timing of *Chl* maxima. Day length increases when the day is closer to the summer solstice (mid-summer). Day length cannot be used as a proxy for timing in the equatorial region where the annual changes in the day length are small, and near the poles where day length is 24 h around midsummer. When comparing the trends detected in year day and the day length, it is important whether the *Chl* maximum is before or after the summer solstice. For example, in the Arctic the annual *Chl* maxima typically occur before midsummer to the south

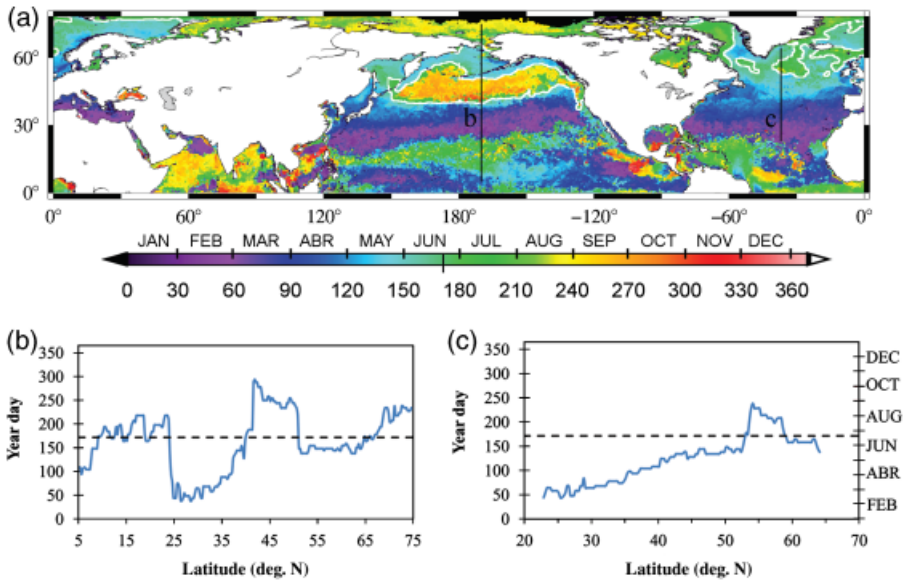

Fig. 1 Median year day of the annual *Chl* maximum for the last 13 years (1997–2009). (a) Northern Hemisphere. The white contours show the transition through the summer solstice (June 20–21, year days 171–172). (b) Transect along 170°W meridian in the North Pacific (black vertical line in a). (c) Transect along 37°W meridian in the North Atlantic (black vertical line in a). The dashed lines in (b and c) show the summer solstice.

of the Bering Strait and after midsummer to the north of the Bering Strait. When the bloom maximum is after the summer solstice (June 20–21, year days 171–172 in Northern Hemisphere), the bloom arriving earlier means that the day length during the bloom is increasing as it is getting closer to the summer solstice. In contrast, when the bloom maximum is before the summer solstice, later blooms are associated with longer day length as the bloom timing is again getting closer to the summer solstice. When *Chl* maxima straddle the summer solstice then the trends in year day and day length are not comparable.

Owing to the high interannual variability in the timing of the annual *Chl* maxima the estimated trends in both year day and the day length of the *Chl* maximum day are noisy and have speckle-like variability (Fig. 2). However, spatially coherent patches of pixels with significant trends are present in certain areas. The trends in the year day of the annual *Chl* maximum are less noisy and easier to interpret in the Arctic where ice cover and low light levels during winter restrict blooms to a relatively narrow time window during boreal summer. In many areas of the Arctic, e.g. the Hudson Bay, Foxe Basin, Baffin Sea, west and east coasts of Greenland, Kara Sea and the Arctic Ocean around Novaya Zemlya, the tendency is for earlier *Chl* maxima (blue colors in Fig. 2a) and longer day length during *Chl* maxima (red colors in Fig. 2b). As the blooms at high latitudes typically occur after the summer solstice, earlier bloom maximum is equivalent to being closer to midsummer; therefore the day length at *Chl* maximum is increasing.

Figures 2c–f give some estimates of the mean rate of change during the last 13 years in selected areas. In some areas, e.g. the Foxe Basin, Baffin and Kara Seas (Fig. 2c–e), the maxima in September (year day ~250) have moved to early July (year day ~200), a change of about 50 days. Earlier bloom maxima are also found in scattered areas elsewhere in the Arctic (e.g. Chukchi Sea, Bothnian Bay in the northernmost Baltic Sea). Similarly, in the huge trans-Pacific zonal band of fall blooms the annual *Chl* maxima have also become earlier (closer to summer solstice) and the corresponding day length has increased. In contrast, in the North Atlantic at mid-latitudes the annual *Chl* maxima (before midsummer) have become later and the corresponding day length has increased. The large changes in the year day of *Chl* maxima in the eastern equatorial Pacific (blue colors in Fig. 2a) are probably due to the strong interannual (ENSO) variability there. As the time series are short and noisy and most detected trends have low statistical significance, we will focus on the Arctic where the trends are easier to interpret and use data outside the Arctic only for comparison.

It is difficult to accurately estimate the area where the trend towards earlier bloom maxima has occurred as clouds and ice severely restrict the availability of ocean color data, especially in the Arctic, but approximately 11% (1.3 million km^2) of the ocean waters north of 60°N with valid *Chl* data show a trend towards

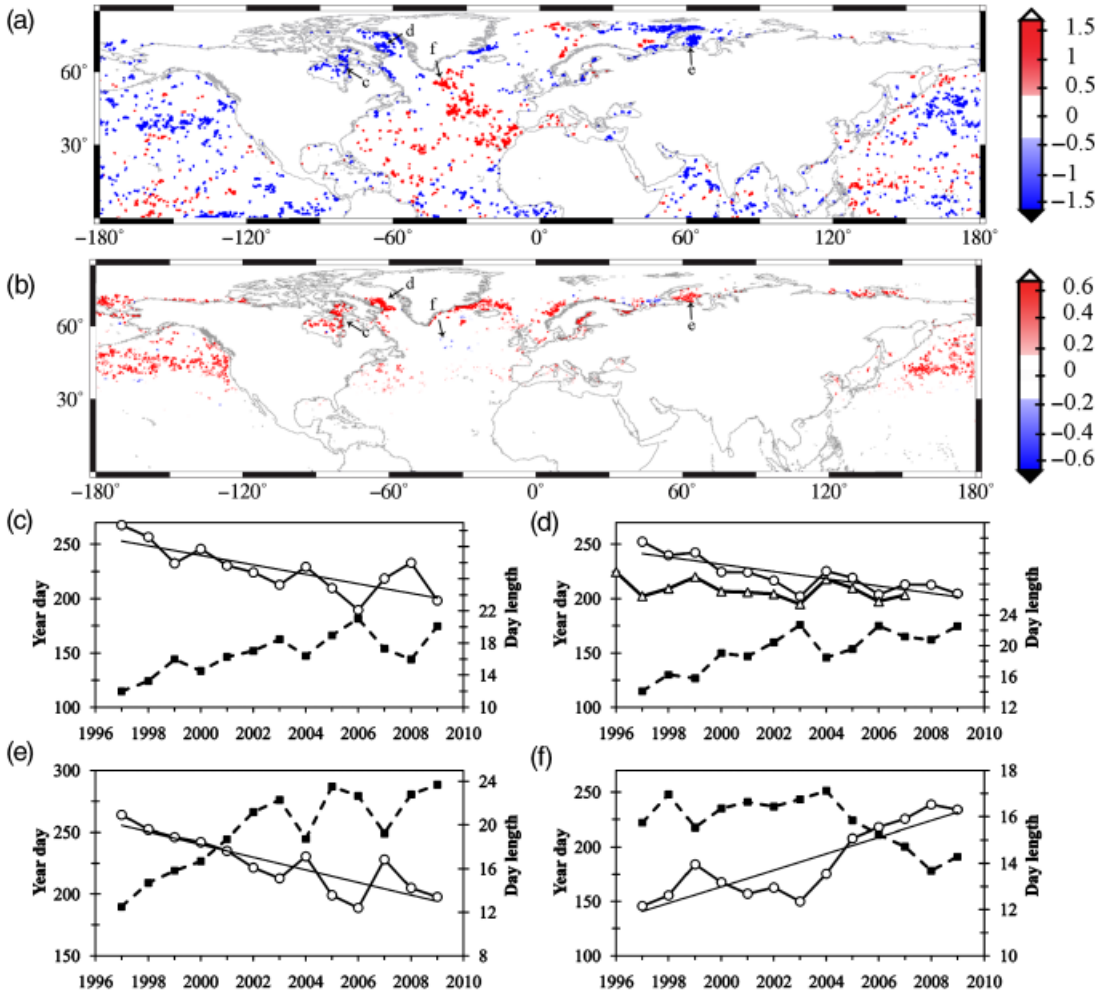

Fig. 2 Detected changes in the timing of the annual *Chl* maximum. (a) Trend (Sen slope) in the year day (YDay) of the annual *Chl* maximum (day/year). (b) Trend (Sen slope) in the day length on the day of the annual *Chl* maximum (hour/year). Red areas show significant (at 95% confidence) increase, blue areas significant decrease while white areas have no significant trend. (c–f) Sample time series of year day (continuous line) and day length (dashed line) showing mean values over N pixels for Foxe Basin (c, YDay $= -4.37X + 8982$, $R^2 = 0.60$, $N = 142$ pixels), Baffin Sea (d, YDay $= -3.31X + 6857$, $R^2 = 0.69$, $N = 178$ pixels), Kara Sea (e, YDay $= -5.10X + 10\ 445$, $R^2 = 0.74$, $N = 284$ pixels) and central North Atlantic (f, YDay $= 7.56X - 14\ 961$, $R^2 = 0.75$, $N = 63$ pixels). Regression lines and parameters are shown for year day (YDay) vs. time (year). The year day when ice concentration becomes $<15\%$ in the Baffin Sea is shown for Fig. 2d (open triangles).

earlier blooms and 1% towards later blooms whereas in approximately 88% of the area no significant trend can be detected.

The spatial pattern of the areas with significant advancement of the phytoplankton bloom shows a striking similarity to the pattern of areas with a significant decrease in early summer (June) ice concentration (Fig. 3). While detailed *in situ* studies are essential in establishing the causal link, it appears that the earlier disappearance of ice is directly related to the earlier start of the phytoplankton bloom maximum. We also evaluated the changes in the length of ice period, the start and end of the ice free period but the results (not shown) were less conclusive. In general, *Chl* maximum follows the disappearance of ice (determined here as the first day of the year with ice concentration $<15\%$) and there is positive correlation between the interannual variability of the timing of the two events but large fluctuations are observed between different areas. In the Baffin Sea (Fig. 2d), the two events are tightly coupled and the time delay between the disappearance of ice and the *Chl* maximum has become smaller.

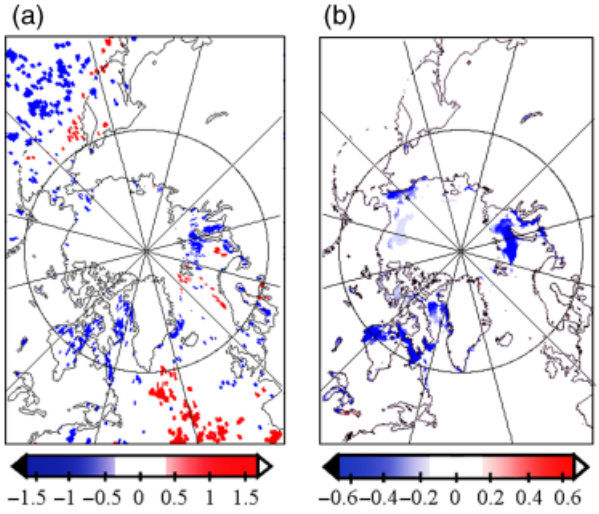

Fig. 3 Comparison of the detected changes in timing of the annual *Chl* maximum (a, day/year, data remapped from Fig. 2a) with trends in early summer (June) ice concentration (b, ice fraction change per year, trend calculated for 1979 to 2007 using monthly ice concentrations from the Nimbus-7 SMMR and DMSP SSM/I passive microwave data).

Discussion

Satellite monitoring of the timing of phytoplankton maxima is subject to errors, primarily because the true maximum may be missed due to cloud cover. Owing to different orbits and changing cloud cover, merged data from multiple satellites have fewer gaps but may be influenced by differences between the satellite sensors and their respective algorithms. Using a single sensor, such as SeaWiFS, is not acceptable as it suffered long periods of data loss in 2008 and 2009 and the useable time series is too short. Satellite estimates of *Chl* in the Arctic are affected by the high concentration of colored dissolved organic matter (CDOM) that is likely to cause errors in the *Chl* estimates using standard algorithms (Matsuoka *et al*., 2007). Fortunately, the metric that we are using, the timing of the *Chl* maximum, is relatively robust and not very sensitive to errors in *Chl* algorithms as CDOM and *Chl* are usually positively correlated. Slight differences in the intercalibration between sensors (Morel *et al*., 2007) are also expected to have a relatively minor influence on estimates of the timing of *Chl* maximum. The reduction in spatial resolution from the sensor's nominal resolution of ~1 km to a pixel size of ~25 km involves several steps of binning and averaging over many level 2 pixels that reduce the error of ~30% in single pixel value of *Chl* (Hu *et al*., 2001). The detection of trends in annual maxima is affected by the significant interannual variability and by the relatively short length of the satellite time series. In spite of these limitations, we have detected statistically significant changes in the timing of the annual *Chl* maxima during the last 13 years. It is important to note that as we are evaluating thousands of pixels using 95% confidence limits, we can expect many (5%) false positives (i.e. type 1 statistical errors). Some of the speckle shown in Figure 2a and b is probably caused by that. However, the fact that some of the pixels with statistically significant trends of earlier *Chl* maxima occur in spatially coherent patches at high latitudes in marginal ice zones, and that approximately the same areas stand out as areas with a significant reduction in early summer ice concentration, supports the idea that the changes towards earlier bloom timing are real and not a coincidence. It is also significant that pixels showing a trend towards later *Chl* maximum are quite rare at high latitudes but dominate, for example, in central North Atlantic (Fig. 3a). Both these facts support the idea that the timing of the annual *Chl* maxima has become significantly earlier in a number of regions in the Arctic. This is likely related to the earlier ice melt in many regions of the Arctic as shown by satellite microwave data. For the period 1979–2007 Markus *et al*. (2009) estimated that the trend towards earlier start of ice melt was up to −7.3 days per decade. The time period that we can use to estimate the rate of change in the timing of phytoplankton bloom maxima is shorter and therefore the estimates are not very accurate. However, it appears that at least in a few selected regions the change in the bloom timing is much faster, about −3 to −5 days per year, i.e. −30 to −50 days per decade (Fig. 2c–e). On the other hand, due to the high variability and relatively short length of the *Chl* time series, small changes in the timing would be difficult to detect statistically even if they existed. The relationship between the timing of ice retreat and the timing of the phytoplankton bloom maximum is not always as simple as it is for the Baffin Sea (Fig. 2d) but rather complex and earlier ice retreat does not necessarily mean earlier phytoplankton bloom. In fact, the opposite relationship exists in the southeastern Bering Sea where winters with no ice or early ice retreat have a delayed spring bloom whereas late ice retreat leads to an early, ice-associated bloom (Hunt *et al*., 2002).

Changes towards earlier *Chl* maxima in boreal Pacific and towards later maxima at mid-latitudes of the North Atlantic (Fig. 2f) are also statistically significant but more difficult to explain. Very few *in situ* studies provide data at scales that are comparable to the satellite data used here. One of the longest time series of *in situ* phytoplankton data (Wiltshire & Manly, 2004) showed that, in the North Sea, warming temperatures were associated with a delay in the annual *Chl* maximum (spring bloom). The trend towards later *Chl* maximum (longer day length at *Chl* maximum) is

also noticeable here for some pixels in the North Sea (Fig. 2b).

The trend towards earlier *Chl* maxima in the Arctic that is detected here using satellite data of 1997–2009 is likely related to the general warming and earlier ice melt in the Arctic (Markus *et al*., 2009; Wang & Overland, 2009). However, with these relatively short time series it is not possible to separate long term effects from interannual variability at decadal scales. For example, the statistically significant trends towards earlier *Chl* maxima in boreal Pacific and later *Chl* maxima in the North Atlantic are more likely to be related to climate cycles such as the Pacific Decadal Oscillation or the North Atlantic oscillation (NAO). Positive NAO phases are known to be associated with stronger westerly winds, deeper mixed layers and lower *Chl* in the North Atlantic (Dickson *et al*., 1988; Boyce *et al*., 2010) that may also lead to delayed *Chl* maxima.

While the advancement in the timing of the phytoplankton bloom cannot continue at the same pace in these areas in the Arctic due to ice cover and light limitation, the trend towards earlier phytoplankton blooms can expand into other areas of the Arctic Ocean and impact the whole food chain. As secondary producers, such as zooplankton and shrimp, may have adapted their reproductive strategy to match the annual phytoplankton bloom (Platt *et al*., 2003; Koeller *et al*., 2009), the match or mismatch with the annual peak in primary production may be critical for the Arctic food webs in their current forms. Short and intense phytoplankton blooms that are not matched by grazing are likely to sink out of the euphotic zone, channel more carbon into the benthic vs. the pelagic communities (Hunt *et al*., 2002), and may cause oxygen deficiency in poorly mixed bottom waters. The potential mismatch of the annual phytoplankton bloom with pelagic grazing as well as the suggested shift towards smaller phytoplankton species (Li *et al*., 2009) may affect the Arctic food web structure and impact the commercially exploited upper trophic level species.

Acknowledgements

Financial support was provided by the NASA Ocean Biology and Biogeochemistry Program and the National Science Foundation. Satellite data were provided by the NASA Ocean Color Processing Group, ESA GlobColour group and the National Snow and Ice Data Center. We thank the anonymous referees for helpful comments on earlier versions of the manuscript.

References

Behrenfeld MJ, O'Malley RT, Siegel DA *et al*. (2006) Climate-driven trends in contemporary ocean productivity. *Nature*, **444**, 752–755.

Boyce DG, Lewis MR, Worm B (2010) Global phytoplankton decline over the past century. *Nature*, **466**, 591–596.

Cavalieri D, Parkinson C, Gloersen P, Zwally HJ (1996, updated 2008) *Sea Ice Concentrations from Nimbus-7 SMMR and DMSP SSM/I Passive Microwave Data, 1990–2007*. National Snow and Ice Data Center. Digital Media, Boulder, CO, USA.

Cleland EE, Chuine I, Menzel A, Mooney HA, Schwartz MD (2007) Shifting plant phenology in response to climate change. *Trends in Ecology and Evolution*, **22**, 357–365.

Cushing DH (1990) Plankton production and year class strength in fish populations: an update of the match/mismatch hypothesis. *Advances in Marine Biology*, **26**, 249–293.

Dickson RR, Kelly PM, Colebrook JM, Wooster WS, Cushing DH (1988) North winds and production in the eastern North Atlantic. *Journal of Plankton Research*, **10**, 151–169.

Djavidnia S, Mélin F, Hoepffner N (2010) Comparison of global ocean colour data records. *Ocean Science*, **6**, 61–76, doi: 10.5194/os-6-61-2010.

Edwards M, Richardson AJ (2004) Impact of climate change on marine pelagic phenology and trophic mismatch. *Nature*, **430**, 881–884.

Gilbert RO (1987) *Statistical Methods for Environmental Pollution Monitoring*. Van Nostrand Reinhold, New York.

Hu C, Carder KL, Muller-Karger FE (2001) How precise are SeaWiFS ocean color estimates? Implications of digitization-noise errors. *Remote Sensing of Environment*, **76**, 239–249.

Hunt GL, Stabeno P, Walters G, Sinclair E, Brodeur RD, Napp JM, Bond NA (2002) Climate change and control of the southeastern Bering Sea pelagic ecosystem. *Deep Sea Research II*, **49**, 5821–5853.

Kahru M, Kudela R, Manzano-Sarabia M, Mitchell BG (2009) Trends in primary production in the California current detected with satellite data. *Journal of Geophysical Research*, **114**, C02004, doi: 10.1029/2008JC004979.

Kahru M, Mitchell BG (2008) Ocean color reveals increased blooms in various parts of the World. *EOS, Transactions, American Geophysical Union*, **89**, 170.

Koeller P, Fuentes-Yaco C, Platt T *et al*. (2009) Basin-scale coherence in phenology of shrimps and phytoplankton in the North Atlantic Ocean. *Science*, **324**, 791–793.

Li WKW, McLaughlin FA, Lovejoy C, Carmack EC (2009) Smallest algae thrive as the Arctic Ocean freshens. *Science*, **326**, 5952–539.

Maritorena S, d'Andon OHF, Mangin A, Siegel DA (2010) Merged satellite ocean color data products using a bio-optical model: characteristics, benefits and issues. *Remote Sensing of the Environment*, **114**, 1791–1804.

Markus T, Stroeve JC, Miller J (2009) Recent changes in Arctic sea ice melt onset, freezeup, and melt season length. *Journal of Geophysical Research*, **114**, C12024, doi: 10.1029/2009JC005436.

Martinez E, Antoine D, D'Ortenzio F, Gentili B (2009) Climate-driven basin-scale decadal oscillations of oceanic phytoplankton. *Science*, **326**, 1253–1256.

Matsuoka A, Huot Y, Shimada K, Saitoh S-I, Babin M (2007) Bio-optical characteristics of the western Arctic Ocean: implications for ocean color algorithms. *Canadian Journal of Remote Sensing*, **33**, 503–518.

Morel A, Huot Y, Gentili B, Werdell PJ, Hooker SB, Franz BA (2007) Examining the consistency of products derived from various ocean color sensors in open ocean (Case 1) waters in the perspective of a multi-sensor approach. *Remote Sensing of Environment*, **111**, 69–88.

Morel A, Maritorena S (2001) Bio-optical properties of oceanic waters: a reappraisal. *Journal of Geophysical Research*, **106**, 7763–7780.

Myneni RB, Keeling CD, Tucker CJ, Asrar G, Nemani RR (1997) Increased plant growth in the northern high latitudes from 1981 to 1991. *Nature*, **386**, 698–702.

O'Reilly JE, Maritorena S, Mitchell BG *et al*. (1998) Ocean color chlorophyll algorithms for SeaWiFS. *Journal of Geophysical Research*, **103**, 24937–24953.

Platt T, Fuentes-Yaco C, Frank KT (2003) Spring algal bloom and larval fish survival. *Nature*, **423**, 398–399.

Platt T, Sathyendranath S, White G, Fuentes-Yaco C, Zhai L, Devred E (2010) Diagnostic properties of phytoplankton time series from remote sensing. *Estuaries and Coasts*, **33**, 428–439.

Salmi T, Määttä A, Anttila P, Ruoho-Airola T, Amnell T (2002) *Detecting trends of annual values of atmospheric pollutants by the Mann–Kendall test and Sen's slope estimates – the Excel template application MAKESENS*. Publications on air quality, **31**, Report Code FMI-AQ-31, ISBN 951-697-563-1, 35pp.

Sen PK (1968) Estimates of the regression coefficient based on Kendall's tau. *Journal of the American Statistical Association*, **63**, 1379–1389.

Siegel DA, Doney SC, Yoder JA (2002) The North Atlantic spring phytoplankton bloom and Sverdrup's critical depth hypothesis. *Science*, **296**, 730–733.

Thackeray SJ, Jones ID, Maberly SC (2008) Long-term change in the phenology of spring phytoplankton: species-specific responses to nutrient enrichment and climatic change. *Journal of Ecology*, **96**, 523–535.

Vargas M, Brown CW, Sapiano MRP (2009) Phenology of marine phytoplankton from satellite ocean color measurements. *Geophysical Research Letters*, **36**, L01608, doi: 10.1029/2008GL036006.

Wang M, Overland JE (2009) A sea ice free summer Arctic within 30 years? *Geophysical Research Letters*, **36**, L07502, doi: 10.1029/2009GL037820.

Wiltshire KH, Manly BFJ (2004) The warming trend at Helgoland Roads, North Sea: phytoplankton response. *Helgoland Marine Research*, **58**, 269–273.

Winder M, Cloern JE (2009) *Does the terrestrial phenology concept apply in water?* American Geophysical Union, Fall Meeting 2009, abstract PA21A-1294.

Winder M, Schindler DE (2004) Climatic effects on the phenology of lake processes. *Global Change Biology*, **10**, 1844–1856.